J. Fluid Mech. (2013), *vol.* 733, R6, doi:10.1017/jfm.2013.476

JFM RAPIDS
journals.cambridge.org/rapids

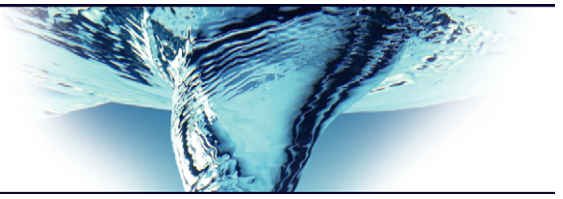

On the rotation of porous ellipsoids in simple shear flows

Hassan Masoud[1,2],†, **Howard A. Stone**[2] **and Michael J. Shelley**[1]

[1]Applied Mathematics Laboratory, Courant Institute of Mathematical Sciences, New York University, NY 10012, USA
[2]Department of Mechanical and Aerospace Engineering, Princeton University, Princeton, NJ 08544, USA

(Received 4 August 2013; revised 4 August 2013; accepted 9 September 2013)

We study theoretically the dynamics of porous ellipsoids rotating in simple shear flows. We use the Brinkman–Debye–Bueche (BDB) model to simulate flow within and through particles and solve the coupled Stokes–BDB equations to calculate the overall flow field and the rotation rate of porous ellipsoids. Our results show that the permeability has little effect on the rotational behaviour of particles, and that Jeffery's prediction of the angular velocity of impermeable ellipsoids in simple shear flows (*Proc. R. Soc. Lond.* A, vol. 102, 1922, pp. 161–179) remains an excellent approximation, if not an exact one, for porous ellipsoids. Employing an appropriate scaling, we also present approximate expressions for the torque exerted on ellipses and spheroids rotating in a quiescent fluid. Our findings can serve as the basis for developing a suspension theory for non-spherical porous particles, or for understanding the orientational diffusion of permeable ellipses and spheroids.

Key words: porous media, rheology, suspensions

1. Introduction

The interaction of flows with porous structures arises in many contexts, such as agglomeration (Vainshtein & Shapiro 2006; Vanni & Gastaldi 2011), chromatography (Deen 1987; Regnier 1991), drug delivery and tissue engineering (Stuart *et al.* 2010; Masoud & Alexeev 2010; Masoud, Bingham & Alexeev 2012), pulp and paper manufacturing (Deng & Dodson 1994), and waste-water treatment (Gujer & Boller 1978). For flow through porous media, Brinkman (1947, 1948) and Debye & Bueche (1948) independently introduced the so-called Brinkman–Debye–Bueche (BDB) model, which includes velocity gradients not present in the more common Darcy (1856) description. Since then, there have been many theoretical studies concerning the flow past rigid porous bodies, including the flow relative to a single object (Adler

† Email address for correspondence: hmasoud@princeton.edu

& Mills 1979; Sonntag & Russel 1987; Zlatanovski 1999; Hsu & Hsieh 2003; Vainshtein, Shapiro & Gutfinger 2004; Cichocki & Felderhof 2009; Ollila, Ala-Nissila & Denniston 2012), flow past two bodies (Reuland, Felderhof & Jones 1978; Yano, Kieda & Mizuno 1991; Richardson & Power 1996), and flow through a swarm of particles (Davis & Stone 1993; Mo & Sangani 1994; Kirsh 2006; Abade *et al.* 2010).

Nonetheless, to the best of our knowledge, there have been no theoretical investigations of the rotational behaviour of non-spherical porous particles. However, the rate at which these objects rotate in fluid flows is important in a number of situations. For instance, the rotation rate of suspended porous particles in linear flows has an impact on the rheology of the suspension. As another example, the release rate of encapsulated drugs from the porous membrane of drug delivery capsules is affected by how fast the capsules rotate in blood flow, which is more pronounced for non-spherical capsules (Ma *et al.* 2008). Moreover, the rotational dynamics of small organisms that are covered with a permeable layer could influence the rate at which they encounter predators in feeding flows (Nguyen *et al.* 2011). As a last example, the rotation rate of flocs, usefully regarded as porous objects, affects their disaggregation in planar linear flow fields (Blaser 2000).

Here, we examine the effect of permeability on the rotation rate of ellipsoids in simple shear flows. We also study the orientational diffusion of porous ellipses and spheroids in dilute suspensions. To this end, we employ a domain integral technique to solve numerically the coupled Stokes–BDB equations. In addition, we perform asymptotic analyses in the limit of large particle permeability.

Our calculations reveal that the flow field inside and around particles significantly depends on the permeability. We show that, surprisingly, this feature has little effect on the rotational dynamics of ellipsoids. Our analyses further indicate that a particular scaling can be exploited to obtain approximate expressions for the orientational diffusion of ellipses and spheroids. In the following, we first describe our methodology and then present our results for rotation rates and orientational diffusion.

2. Methodology

2.1. *Governing equations*

Consider simple shear flow past a torque-free, force-free ellipsoid rotating with an unknown angular velocity $\boldsymbol{\omega}$. The undisturbed flow field is $\boldsymbol{u}^{\infty} = \Gamma\,(\boldsymbol{r}\cdot\boldsymbol{n})\,\boldsymbol{\ell}$, where $\boldsymbol{r}$ is the position vector, Γ is the shear rate, and $\boldsymbol{\ell}$ and $\boldsymbol{n}$ are, respectively, unit vectors in the direction of the streamlines and velocity gradient that determine the relative orientation of ellipsoid and shear flow. The xyz coordinate system coincides with the principal axes of the ellipsoid whose semi-lengths are, respectively, a, b, and c.

Let $\boldsymbol{\sigma} = -p\boldsymbol{I} + 2\mu\boldsymbol{E}$ be the usual stress tensor for an incompressible flow of a Newtonian fluid (viscosity μ) with velocity $\boldsymbol{u}$, pressure p, and symmetric rate-of-strain tensor $\boldsymbol{E} = [\boldsymbol{\nabla u} + (\boldsymbol{\nabla u})^{\mathrm{T}}]/2$. Then, according to the BDB model, the inertialess fluid flow inside the particle is governed by the equations

$$\boldsymbol{\nabla}\cdot\boldsymbol{u} = 0 \quad \text{and} \quad \boldsymbol{\nabla}\cdot\boldsymbol{\sigma} \equiv \mu\nabla^2\boldsymbol{u} - \boldsymbol{\nabla}p = \mu k^{-1}\left(\boldsymbol{u} - \boldsymbol{u}_p\right), \tag{2.1}$$

whereas outside the particle the flow obeys the Stokes equations

$$\boldsymbol{\nabla}\cdot\boldsymbol{u} = 0 \quad \text{and} \quad \boldsymbol{\nabla}\cdot\boldsymbol{\sigma} \equiv \mu\nabla^2\boldsymbol{u} - \boldsymbol{\nabla}p = \boldsymbol{0}. \tag{2.2}$$

The right-hand side of (2.1) represents the drag experienced by the solid skeleton of the porous particle due to motion relative to the surrounding fluid, where k is the Darcy permeability and $\boldsymbol{u}_p$ is the velocity of the particle skeleton. It has been shown

that the BDB model accurately represents the Stokes flow through porous objects with low solid volume fractions whose characteristic lengths are much larger than their average pore size (see for example Durlofsky & Brady 1987). In our problem $\boldsymbol{u}_p = \boldsymbol{\omega} \times \boldsymbol{r}$. The BDB and Stokes equations are coupled through the continuity of velocity and traction forces at the particle surface. Additionally, the flow approaches the free stream $\boldsymbol{u} \to \boldsymbol{u}^\infty$ as $|\boldsymbol{r}| \to \infty$.

Inspection of (2.1) and (2.2) reveals that the flow past a porous particle can be viewed as a Stokes flow with a distribution of body force $-\mu k^{-1}(\boldsymbol{u} - \boldsymbol{u}_p)$ within the particle volume V_p. Hence, the velocity everywhere, both inside and outside, can be written in terms of the Green's function (or Stokeslet) as

$$\boldsymbol{u}(\boldsymbol{r}) = \boldsymbol{u}^\infty(\boldsymbol{r}) - \int_{V_p} \boldsymbol{G}(\boldsymbol{r}, \boldsymbol{r}_0) \cdot k^{-1} \left[\boldsymbol{u}(\boldsymbol{r}_0) - \boldsymbol{u}_p(\boldsymbol{r}_0)\right] \, \mathrm{d}V_{\boldsymbol{r}_0} \tag{2.3}$$

(Felderhof 1975; Higdon & Kojima 1981) where in two dimensions we have

$$\boldsymbol{G}(\boldsymbol{r}, \boldsymbol{r}_0) = \frac{1}{4\pi} \left[\frac{\boldsymbol{I}}{\ln |\boldsymbol{r} - \boldsymbol{r}_0|} + \frac{(\boldsymbol{r} - \boldsymbol{r}_0)\,(\boldsymbol{r} - \boldsymbol{r}_0)}{|\boldsymbol{r} - \boldsymbol{r}_0|^2} \right] \tag{2.4}$$

and in three dimensions,

$$\boldsymbol{G}(\boldsymbol{r}, \boldsymbol{r}_0) = \frac{1}{8\pi} \left[\frac{\boldsymbol{I}}{|\boldsymbol{r} - \boldsymbol{r}_0|} + \frac{(\boldsymbol{r} - \boldsymbol{r}_0)\,(\boldsymbol{r} - \boldsymbol{r}_0)}{|\boldsymbol{r} - \boldsymbol{r}_0|^3} \right]. \tag{2.5}$$

Here, $\boldsymbol{G}(\boldsymbol{r}, \boldsymbol{r}_0) \cdot (\boldsymbol{\alpha}/\mu)$ is the fluid velocity at the position $\boldsymbol{r}$ due to a point force $\boldsymbol{\alpha}$ applied at the position $\boldsymbol{r}_0$ (Pozrikidis 1992). We allow the permeability k to be non-uniform and, therefore, keep it inside the integral. According to (2.1), the force and torque (with respect to the origin) experienced by the particle are, respectively,

$$\boldsymbol{F} = \mu \int_{V_p} k^{-1} \left(\boldsymbol{u} - \boldsymbol{u}_p\right) \, \mathrm{d}V \tag{2.6}$$

and

$$\boldsymbol{T} = \mu \int_{V_p} \boldsymbol{r} \times k^{-1} \left(\boldsymbol{u} - \boldsymbol{u}_p\right) \, \mathrm{d}V. \tag{2.7}$$

2.2. *Solution strategy*

Jeffery (1922) determined $\boldsymbol{\omega}$ analytically for impermeable ellipsoids (i.e. Jeffery solved the flow problem in the limit of $k \to 0$). A natural question is whether these classical results can be extended to porous ellipsoids. To answer this question we need to determine at what angular velocity $\boldsymbol{\omega}$ the porous ellipsoid experiences no net torque (the force-free condition is met due to the symmetry).

We begin by writing the velocity as a superposition of four flows,

$$\boldsymbol{u} = \boldsymbol{\omega} \times \boldsymbol{r} + \tilde{\boldsymbol{u}}_{xy} + \tilde{\boldsymbol{u}}_{xz} + \tilde{\boldsymbol{u}}_{yz}, \tag{2.8}$$

where $\tilde{\boldsymbol{u}}_{xy}$, $\tilde{\boldsymbol{u}}_{xz}$, and $\tilde{\boldsymbol{u}}_{yz}$ are, respectively, the solutions of the coupled Stokes–BDB equations for shear flows $\tilde{\boldsymbol{u}}^\infty_{xy}$, $\tilde{\boldsymbol{u}}^\infty_{xz}$, and $\tilde{\boldsymbol{u}}^\infty_{yz}$ past a stationary ellipsoid ($\boldsymbol{u}_p = \boldsymbol{0}$). Here,

$$\tilde{\boldsymbol{u}}^\infty_{xy} = [\Gamma(n_2\ell_1 y - n_2\ell_2 x) + \omega_3 y]\boldsymbol{e}_x + [\Gamma(n_2\ell_2 y + n_1\ell_2 x) - \omega_3 x]\boldsymbol{e}_y, \tag{2.9a}$$

$$\tilde{\boldsymbol{u}}^\infty_{xz} = [\Gamma(n_3\ell_1 z - n_3\ell_3 x) - \omega_2 z]\boldsymbol{e}_x + [\Gamma(n_3\ell_3 z + n_1\ell_3 x) + \omega_2 x)]\boldsymbol{e}_z, \tag{2.9b}$$

$$\tilde{\boldsymbol{u}}^\infty_{yz} = (\Gamma n_3\ell_2 + \omega_1) z\boldsymbol{e}_y + (\Gamma n_2\ell_3 - \omega_1) y\boldsymbol{e}_z. \tag{2.9c}$$

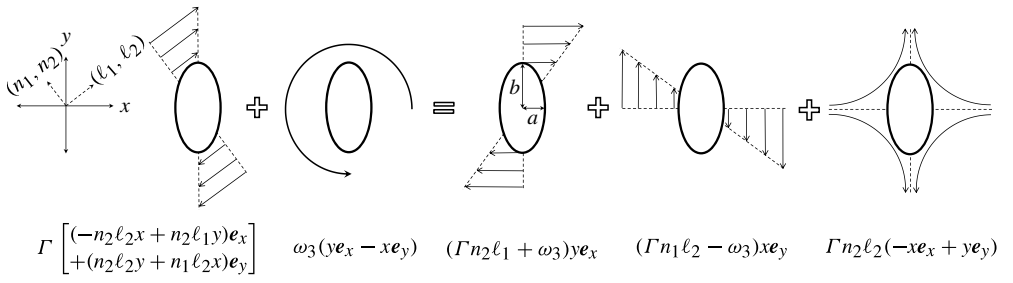

FIGURE 1. Schematic illustrating the decomposition of the incident flow $\tilde{\boldsymbol{u}}^{\infty}_{xy}$. From left to right, the depicted incident flows are simple shear with the velocity gradient in the direction of (n_1, n_2), pure rotational flow, simple shear with the velocity gradient in the y-direction, simple shear with the velocity gradient in the x-direction, and pure extensional flow with symmetry axes in the x- and y-directions. Here, n_3 and ℓ_3 are set to zero.

We require that the summation of torques applied by these four flows (including $\boldsymbol{\omega} \times \boldsymbol{r}$) be zero. First, the rigid-body rotation does not exert a torque on the particle. Moreover, the flows $\tilde{\boldsymbol{u}}_{xy}$, $\tilde{\boldsymbol{u}}_{xz}$, and $\tilde{\boldsymbol{u}}_{yz}$ exert torques in the z-, y-, and x-directions, respectively. Hence, requiring that the torques applied by these flows are individually zero leads to three independent equations for ω_1, ω_2, and ω_3.

Consider first the torque due to $\tilde{\boldsymbol{u}}^{\infty}_{xy}$. Referring to figure 1, this flow can be considered as a superposition of a simple shear flow whose velocity gradient at infinity is in the y-direction, a simple shear whose velocity gradient at infinity is in the x-direction, and a pure extensional flow whose symmetry axes coincide with the x- and y-directions. No net torque is produced as a result of the extensional flow. Thus, the simple shears yield equal and oppositely signed torques.

Denoting the absolute value of torques on a stationary ellipsoid due to $\tilde{\boldsymbol{u}}^{\infty} = y\boldsymbol{e}_x$ and $\tilde{\boldsymbol{u}}^{\infty} = x\boldsymbol{e}_y$ by T^y_x and T^x_y, respectively, we have

$$\omega_3 = \Gamma \left(n_1\ell_2 \frac{T^x_y}{T^y_x + T^x_y} - n_2\ell_1 \frac{T^y_x}{T^y_x + T^x_y} \right). \tag{2.10a}$$

Following the same procedure, it can be shown that

$$\omega_2 = \Gamma \left(n_3\ell_1 \frac{T^z_x}{T^z_x + T^x_z} - n_1\ell_3 \frac{T^x_z}{T^z_x + T^x_z} \right) \tag{2.10b}$$

and

$$\omega_1 = \Gamma \left(n_2\ell_3 \frac{T^y_z}{T^y_z + T^z_y} - n_3\ell_2 \frac{T^z_y}{T^y_z + T^z_y} \right), \tag{2.10c}$$

where T^z_x, T^x_z, T^z_y and T^y_z are the absolute value of torques required to hold the ellipsoid fixed when $\tilde{\boldsymbol{u}}^{\infty} = z\boldsymbol{e}_x$, $\tilde{\boldsymbol{u}}^{\infty} = x\boldsymbol{e}_z$, $\tilde{\boldsymbol{u}}^{\infty} = z\boldsymbol{e}_y$ and $\tilde{\boldsymbol{u}}^{\infty} = y\boldsymbol{e}_z$, respectively.

Equations (2.10a)–(2.10c) demonstrate that the problem of finding the rotation rate $\boldsymbol{\omega}$ of an ellipsoid at any orientation in a simple shear flow reduces to finding three dimensionless parameters T^y_x/T^x_y, T^z_x/T^x_z and T^z_y/T^y_z. So, for example, to calculate ω_3, we need only solve the flow past a fixed ellipsoid due to $\tilde{\boldsymbol{u}}^{\infty} = y\boldsymbol{e}_x$ and $\tilde{\boldsymbol{u}}^{\infty} = x\boldsymbol{e}_y$.

The torque ratios of an impermeable ellipsoid are simply equal to the square of the corresponding axis ratios (Jeffery 1922; Bretherton 1962):

$$\frac{T_x^y}{T_y^x} = \left(\frac{b}{a}\right)^2, \quad \frac{T_x^z}{T_z^x} = \left(\frac{c}{a}\right)^2, \quad \frac{T_y^z}{T_z^y} = \left(\frac{c}{b}\right)^2. \tag{2.11}$$

For a porous ellipsoid, on the other hand, one would expect the torque ratios to be not only a function of the geometry but also a function of the particle permeability. To the contrary, we find that the torque ratios of a highly permeable homogeneous ellipsoid are the same as those of an impermeable one. This result can be shown analytically since $\boldsymbol{u} \to \boldsymbol{u}^\infty$ as $k \to \infty$, which in conjunction with (2.7) leads to

$$\frac{T_x^y}{T_y^x} = \frac{(4\pi\mu/15k)\, ab^3c}{(4\pi\mu/15k)\, a^3bc} = \left(\frac{b}{a}\right)^2, \tag{2.12a}$$

$$\frac{T_x^z}{T_z^x} = \frac{(4\pi\mu/15k)\, abc^3}{(4\pi\mu/15k)\, a^3bc} = \left(\frac{c}{a}\right)^2, \tag{2.12b}$$

$$\frac{T_y^z}{T_z^y} = \frac{(4\pi\mu/15k)\, abc^3}{(4\pi\mu/15k)\, ab^3c} = \left(\frac{c}{b}\right)^2. \tag{2.12c}$$

To verify whether this is the case for intermediate permeabilities, we seek a numerical solution of (2.3).

2.3. *Numerical approach*

Equation (2.3) is an inhomogeneous Fredholm integral equation of the second kind with a weakly singular kernel $\boldsymbol{G}(\boldsymbol{r}, \boldsymbol{r}_0)$ (Pozrikidis 1992). To solve this equation numerically, we first discretize the integration domain into a uniform distribution of N cubic (square in two dimensions) elements whose centres lie inside the domain boundary. Despite its simplicity, our calculations (not shown here) indicate that this discretization provides results comparable to those obtained using boundary-fitted grids. We then approximate the integral on the right-hand side of (2.3) by

$$\int_{V_p} \boldsymbol{G}(\boldsymbol{r}, \boldsymbol{r}_0) \cdot k^{-1}\boldsymbol{u}(\boldsymbol{r}_0)\, \mathrm{d}V_{\boldsymbol{r}_0} = \sum_{i=1}^{N} \left[k^{-1}\boldsymbol{u}(\boldsymbol{r}_i) \cdot \int_{V_i} \boldsymbol{G}(\boldsymbol{r}, \boldsymbol{r}_0)\, \mathrm{d}V_{\boldsymbol{r}_0} \right], \tag{2.13}$$

where V_i and $\boldsymbol{r}_i$ represent the volume and location of the centre of the ith cubic element, respectively. Here, it is assumed that $k^{-1}\boldsymbol{u}$ is constant over each element. Where possible, the integral of the Stokeslet over elements is carried out analytically. Otherwise, an adaptive quadrature is used to evaluate the integral. This quadrature satisfies at least one of the following conditions: (i) absolute error $\leqslant 10^{-10}$; (ii) relative error $\leqslant 10^{-6}$.

Next, we enforce the integral equation (2.3) at the centre of elements located in the first octant (quadrant in two dimensions) of the coordinate system. This results in a set of linear equations to be solved for the fluid velocity $\boldsymbol{u}(\boldsymbol{r}_i)$; the velocity in other octants (quadrants) is related to the velocity in the first octant (quadrant) by virtue of the flow symmetry. We solve the linear system of equations using the LU factorization with partial pivoting and, finally, we calculate the torque exerted on the particle using

$$\boldsymbol{T} = \mu \sum_{i=1}^{N} V_i \boldsymbol{r}_i \times k^{-1}\boldsymbol{u}(\boldsymbol{r}_i). \tag{2.14}$$

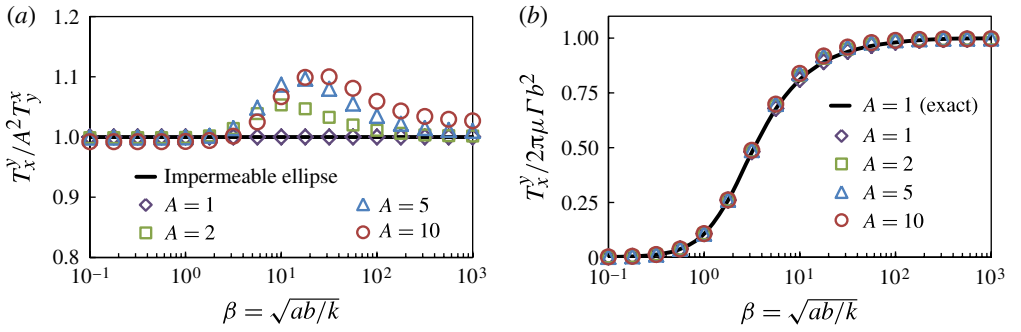

FIGURE 2. Simple shear flow past stationary ellipses of various axis ratios $A = b/a$. (*a*) Normalized torque ratio $T_x^y/A^2T_y^x$ and (*b*) dimensionless torque $T_x^y/2\pi\mu\Gamma b^2$ as a function of the dimensionless permeability $\beta = \sqrt{ab/k}$.

We note that since $\boldsymbol{G}(\boldsymbol{r}, \boldsymbol{r}_0) = \boldsymbol{G}(\boldsymbol{r}_0, \boldsymbol{r})$, the coefficient matrix of the system of equations is symmetric.

In all of our two- and three-dimensional calculations, we set the number of elements in each octant and quadrant to approximately $N \approx 2000$. To validate our domain integral technique, we calculate the torque applied on a sphere and circle in a simple shear flow and compare our results with the corresponding analytical solutions (see the Appendix). In both cases the relative error at all permeabilities is less than 1 %.

3. Results and discussion

We first consider the two-dimensional problem of the torque ratio of ellipses with various axis ratios $A = b/a$. Figure 2 shows our results for the normalized torque ratio $T_x^y/A^2T_y^x$ and dimensionless torque $T_x^y/2\pi\mu\Gamma b^2$ as a function of the dimensionless permeability $\beta = \sqrt{ab/k}$. We observe that the torque ratio is a weak function of the permeability (figure 2*a*). Consistent with our asymptotic analysis and Jeffery's calculations, normalized torque ratios approach unity in both the highly permeable ($\beta < 1$) and impermeable ($\beta > 100$) limits. At intermediate values of β, however, we observe a small deviation from unity. The maximum deviation occurs at $\beta \approx 20$ and is less than 10 % for all values of A considered.

In addition, we find that the curves of dimensionless torque versus dimensionless permeability for ellipses of different axis ratios are practically overlapping (see figure 2*b*) indicating that the torque exerted on an ellipse by the shear flow is very well approximated by the torque on the circle with radius b

$$T_x^y \approx 2\pi\mu\Gamma b^2 \frac{I_2(\beta)}{I_0(\beta)} \tag{3.1}$$

where I_0 and I_2 are modified Bessel functions of the first kind (see (A 4)). Given the above equation and the fact that the torque ratio $T_x^y/T_y^x \approx A^2$ (figure 2*a*), we estimate the torque experienced by an ellipse rotating with an angular velocity ω_3 in a quiescent fluid as

$$\boldsymbol{T} = -\omega_3 \left(T_y^x + T_x^y\right) \boldsymbol{e}_z \approx -2\pi\mu\omega_3 \left(a^2 + b^2\right) \frac{I_2(\beta)}{I_0(\beta)} \boldsymbol{e}_z. \tag{3.2}$$

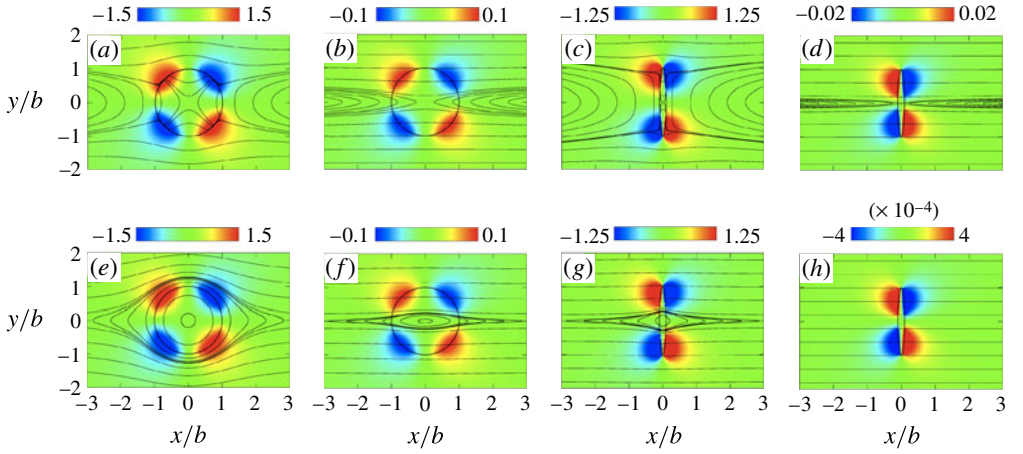

FIGURE 3. Streamlines and dimensionless pressure distributions $p/\mu\Gamma$ from the domain integral solutions for simple shear flows past (*a–d*) fixed and (*e–h*) freely rotating circles (left-hand plots)and ellipses of axis ratio $A = 10$ (right-hand plots). Dimensional permeability of particles in (*a,c,e,g*) is $k = 100b^2$ whereas particles in (*b,d,f,h*) have $k = b^2$.

Equation (3.2) in conjunction with the Stokes–Einstein–Sutherland relation for the rotational diffusivity provides an estimation for the rotational diffusion of porous ellipses in dilute solutions.

To gain better insight into the flow pattern inside and around fixed and freely rotating porous particles in a simple shear flow, we plot streamlines and pressure contours for flows past a circle and an ellipse of axis ratio $A = 10$ (see figure 3). We present these results for two particles with permeabilities $k/b^2 = 1, 100$. Figure 3 confirms our initial intuition regarding the strong influence of permeability on the flow field interior and exterior to the particle. However, as illustrated by figure 2(*a*), this flow feature does not necessitate an equally strong influence on the torque ratio. Figure 3 also shows that for two particles sharing the same permeability, the thinner ellipse allows more streamlines to pass through, i.e. the more slender particles are effectively more permeable. This result explains the collapse of the data when the permeability is non-dimensionalized by ab instead of b^2 or a^2.

Next, consider prolate spheroids whose symmetry axes are in the y-direction ($a = c$). Our calculations reveal that the variation of the torque ratios as a function of the dimensionless permeability is similar to those of ellipses (see figure 4*a*), again showing the weak effect of permeability on the rotation rate. Our calculations also indicate that the dimensionless torque $T_x^y/4\pi\mu\Gamma b^3$ does not scale uniformly with the axis ratio A for all values of β. Therefore, we rescale it differently in the highly permeable and impermeable limits according to (2.12*a*) and the results of Jeffery (1922). Figures 4(*b*) and 4(*c*) show that a good collapse of data is obtained in this manner. Thus, we approximate the torque required to hold a prolate spheroid fixed in a shear flow by (see also (A 1))

$$T_x^y \approx 4\pi\mu\Gamma b^2 c \left(\frac{\beta^2 + 3 - 3\beta\coth\beta}{\beta^2}\right) \quad \text{for } \beta \lesssim 1 \tag{3.3a}$$

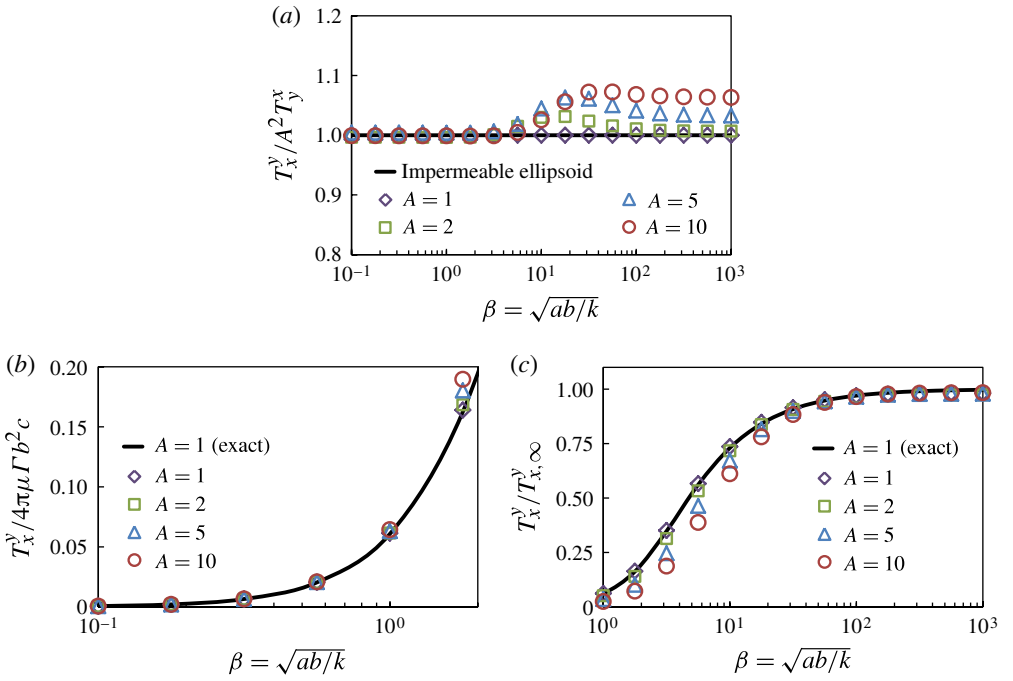

FIGURE 4. Simple shear flow past stationary prolate spheroids of various axis ratios $A = b/a$. (*a*) Normalized torque ratio $T_x^y/A^2T_y^x$ as a function of the dimensionless permeability $\beta = \sqrt{ab/k}$. (*b*) Dimensionless torque $T_x^y/4\pi\mu\Gamma b^2 c$ versus dimensionless permeability for $\beta < 2$. (*c*) Dimensionless torque $T_x^y/T_{x,\infty}^y$ versus dimensionless permeability for $\beta \geqslant 1$. $T_{x,\infty}^y$ is the torque experienced by an impermeable spheroid.

and

$$T_x^y \approx T_{x,\infty}^y \left(\frac{\beta^2 + 3 - 3\beta \coth \beta}{\beta^2} \right) \quad \text{for } \beta \gtrsim 10 \tag{3.3b}$$

where $T_{x,\infty}^y$ is the torque experienced by an impermeable spheroid (Jeffery 1922). T_x^y in the range $1 < \beta < 10$ can be well approximated by the linear interpolation of (3.3*a*) and (3.3*b*).

We note that (3.3*a*) and (3.3*b*) are also applicable to oblate spheroids with the axis of symmetry in the x-direction ($b = c$). Additionally, the computation of T_x^y and T_y^x for oblate spheroids (not shown here) indicates that the change in the torque ratios as a result of a change in the dimensionless permeability is similar to that already observed for ellipses and prolate spheroids. Needless to say, (3.3*a*) and (3.3*b*) can be used to estimate the orientational diffusion of porous spheroids (see (3.2) and the accompanying explanation).

Taking the results so far obtained into consideration, we are now in a position to answer the question we posed earlier in § 2.2. Our calculations, asymptotic and numerical, demonstrate that, independent of c, the torque ratio T_x^y/T_y^x scales with the square of the axis ratio $A^2 = (b/a)^2$ and is largely insensitive to the permeability k. Hence, Jeffery's results for the rotation rate of impermeable ellipsoids in simple shear flows apply very closely to porous ellipsoids. This statement is further supported by the experiments of Blaser (2000) who examined the rotation rate of preflocculated

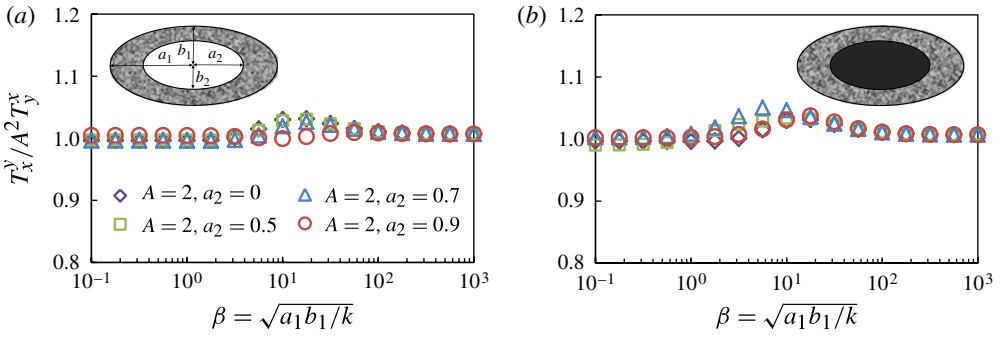

FIGURE 5. Simple shear flow past stationary prolate (*a*) hollow and (*b*) core–shell spheroids of axis ratio $A = 2$: normalized torque ratio $T_x^y/A^2T_y^x$ as a function of dimensionless permeability $\beta = \sqrt{a_1 b_1/k}$. a_1 (a_2) and b_1 (b_2) are the semi-minor and semi-major axes of the outer (inner) spheroid, respectively. The dark colour in (*b*) represents the impermeable region.

ferric hydroxide flocs in a simple shear flow. According to these measurements, the rotation rate of highly porous objects is well approximated by Jeffery's results.

We extend our results by examining the torque ratio of hollow and core–porous shell prolate spheroids (see figure 5). We denote the semi-minor and semi-major axes of the outer (inner) spheroid by a_1 (a_2) and b_1 (b_2), respectively. Hollow spheroids can be perceived as models for non-spherical drug delivery capsules made of porous polymer networks (Ma *et al.* 2008; Masoud & Alexeev 2012) whereas core–shell particles may be considered as models for impermeable particles coated with a layer of polymer brush (Cichocki & Felderhof 2009; Stuart *et al.* 2010) or for ciliated organisms (Keller & Wu 1977; Nguyen *et al.* 2011).

We compute the flow through hollow spheroids by limiting the domain of integration in (2.3) to the porous shell. To calculate the flow past core–shell spheroids, we fix the permeability of elements in the impermeable core to $k = 10^{-3}a_1 b_1$; note that in our domain integral formulation permeability can be specified locally, thereby enabling us to handle non-uniformities in k. Here, we set the axis ratio to $A = 2$ and change the thickness of the porous layer. We find that the torque ratio curves for these inhomogeneous porous particles resemble those obtained for uniformly porous spheroids, which indicates the insensitivity of the torque ratio to not only the permeability but also the thickness of the porous layer (see figure 5).

4. Conclusion

We examined the rotational behaviour of porous ellipsoids in simple shear flows and showed that the angular velocity of freely rotating ellipsoids about each principal axis at any orientation relative to the plane of shear depends only on one dimensionless parameter, namely, the corresponding torque ratio. Our asymptotic analysis revealed that the torque ratios for highly permeable ellipsoids are identical to those for impermeable ones. Moreover, our numerical analyses using a domain integral technique demonstrated that the torque ratios at intermediate permeabilities deviate only slightly (less than 10 %) from the asymptotic values. These findings indicate that the angular velocity of a porous ellipsoid can be calculated to a very good approximation using Jeffery's results for an impermeable ellipsoid in shear

flow. Further, we showed that this result may even apply to inhomogeneous porous ellipsoids such as hollow and core–shell porous spheroids. Finally, we provided estimates for the torque experienced by ellipses and spheroids rotating in a quiescent fluid, which can be readily used to approximate their orientational diffusion in dilute solutions.

Acknowledgements

H.M. and M.J.S. were supported by DOE grant DE-FG02-88ER25053. H.M. acknowledges support from NSF grant DMR-0844115 and the Institute for Complex Adaptive Matter. H.A.S. acknowledges support from NSF grant CBET-1234500.

Appendix

The torque exerted by a simple shear flow of strength Γ on a fixed porous sphere (or circle) is equal to the torque experienced by a sphere (or circle) rotating with an angular velocity $\Gamma/2$ in a quiescent fluid. Felderhof (1975) analytically solved for the Stokes flow around a porous sphere rotating with velocity $\boldsymbol{u}_p = \omega_3 \boldsymbol{e}_z \times \boldsymbol{r}$ and found

$$\boldsymbol{T} = -8\pi\mu\omega_3 b^3 \left(\frac{\beta^2 + 3 - 3\beta \coth \beta}{\beta^2} \right) \boldsymbol{e}_z, \tag{A 1}$$

where b is the sphere radius and $\beta = b/\sqrt{k}$. Yang & Hong (1988) used a singularity method to solve the same problem.

To the best of our knowledge, the problem of flow around a rotating porous circle has not been considered before. Therefore, we provide the analytical solution here. Following Yang & Hong (1988), we express the velocity inside and outside the porous circle of radius b in terms of the fundamental solutions of, respectively, the BDB and Stokes equations:

$$\boldsymbol{u} = \omega_3 \boldsymbol{e}_z \times \boldsymbol{r} + \boldsymbol{u}_{RN} = \omega_3 \boldsymbol{e}_z \times \boldsymbol{r} + \frac{I_1\left(|\boldsymbol{r}|/\sqrt{k}\right)}{|\boldsymbol{r}|/\sqrt{k}} \gamma_i \boldsymbol{e}_z \times \boldsymbol{r} \quad \text{for } |\boldsymbol{r}| \leqslant b \tag{A 2a}$$

and

$$\boldsymbol{u} = \boldsymbol{u}_R = \frac{\gamma_o \boldsymbol{e}_z \times \boldsymbol{r}}{|\boldsymbol{r}|^2} \quad \text{for } |\boldsymbol{r}| > b. \tag{A 2b}$$

Here, $\boldsymbol{u}_R$ is the rotlet and $\boldsymbol{u}_{RN}$ is the equivalent of the roton (Chwang & Wu 1975) for the BDB equation. Also, γ_i and γ_o are unknown coefficients and I_0 and I_2 are modified Bessel functions of the first kind. Applying continuity of the velocity and traction forces at the circle boundary, we find

$$\gamma_i = -\frac{2\omega_3}{I_0(\beta)}, \quad \gamma_o = \omega_3 b^2 \frac{I_2(\beta)}{I_0(\beta)}. \tag{A 3}$$

Having determined the strength of the rotlet, the torque experienced by the circle can be calculated as (Chwang & Wu 1975)

$$\boldsymbol{T} = -4\pi\mu\gamma_o \boldsymbol{e}_z = -4\pi\mu\omega_3 b^2 \frac{I_2(\beta)}{I_0(\beta)} \boldsymbol{e}_z. \tag{A 4}$$

References

ABADE, G. C., CICHOCKI, B., EKIEL-JEZEWSKA, M. L., NAGELE, G. & WAJNRYB, E. 2010 High-frequency viscosity of concentrated porous particles suspensions. *J. Chem. Phys.* **133**, 084906.

ADLER, P. M. & MILLS, P. M. 1979 Motion and rupture of a porous sphere in a linear flow field. *J. Rheol.* **23**, 25–37.

BLASER, S. 2000 Flocs in shear and strain flows. *J. Colloid Interface Sci.* **225**, 273–284.

BRETHERTON, F. P. 1962 The motion of rigid particles in a shear flow at low Reynolds number. *J. Fluid Mech.* **14**, 284–304.

BRINKMAN, H. C. 1947 A calculation of the viscous force exerted by a flowing fluid on a dense swarm of particles. *Appl. Sci. Res.* A **1**, 27–34.

BRINKMAN, H. C. 1948 On the permeability of media consisting of closely packed porous particles. *Appl. Sci. Res.* A **1**, 81–86.

CHWANG, A. T. & WU, T. Y. T. 1975 Hydromechanics of low-Reynolds-number flow. Part 2. Singularity method for Stokes flows. *J. Fluid Mech.* **67**, 787–815.

CICHOCKI, B. & FELDERHOF, B. U. 2009 Hydrodynamic friction coefficients of coated spherical particles. *J. Chem. Phys.* **130**, 164712.

DARCY, H. 1856 *Les Fontaines Publiques de la Ville de Dijon: Exposition et Application*. Victor Dalmont.

DAVIS, R. H. & STONE, H. A. 1993 Flow through beds of porous particles. *Chem. Engng Sci.* **48**, 3993–4005.

DEBYE, P. & BUECHE, A. M. 1948 Intrinsic viscosity, diffusion, and sedimentation rate of polymers in solution. *J. Chem. Phys.* **16**, 573–579.

DEEN, W. M. 1987 Hindered transport of large molecules in liquid-filled pores. *AIChE J.* **33**, 1409–1425.

DENG, M. & DODSON, C. T. J. 1994 Random star patterns and paper formation. *Tappi J.* **77**, 195–199.

DURLOFSKY, L. & BRADY, J. F. 1987 Analysis of the Brinkman equation as a model for flow in porous-media. *Phys. Fluids* **30**, 3329–3341.

FELDERHOF, B. U. 1975 Frictional properties of dilute polymer solutions: III. Translational friction coefficient. *Physica* A **80**, 63–75.

GUJER, W. & BOLLER, M. 1978 Basis for the design of alternative chemical-biological waste-water treatment processes. *Prog. Water Technol.* **10**, 741–758.

HIGDON, J. J. L. & KOJIMA, M. 1981 On the calculation of Stokes flow past porous particles. *Intl J. Multiphase Flow* **7**, 719–727.

HSU, J. P. & HSIEH, Y. H. 2003 Drag force on a porous, non-homogeneous spheroidal floc in a uniform flow field. *J. Colloid Interface Sci.* **259**, 301–308.

JEFFERY, G. B. 1922 The motion of ellipsoidal particles in a viscous fluid. *Proc. R. Soc. Lond.* A **102**, 161–179.

KELLER, S. R. & WU, T. Y. 1977 Porous prolate-spheroidal model for ciliated microorganisms. *J. Fluid Mech.* **80**, 259–278.

KIRSH, V. A. 2006 Stokes flow past periodic rows of porous cylinders. *Theor. Found. Chem. Engng* **40**, 465–471.

MA, M. Y., ZHU, Y. J., LI, L. & CAO, S. W. 2008 Nanostructured porous hollow ellipsoidal capsules of hydroxyapatite and calcium silicate: preparation and application in drug delivery. *J. Mater. Chem.* **18**, 2722–2727.

MASOUD, H. & ALEXEEV, A. 2010 Permeability and diffusion through mechanically deformed random polymer networks. *Macromolecules* **43**, 10117–10122.

MASOUD, H. & ALEXEEV, A. 2012 Controlled release of nanoparticles and macromolecules from responsive microgel capsules. *ACS Nano* **6**, 212–219.

MASOUD, H., BINGHAM, B. I. & ALEXEEV, A. 2012 Designing maneuverable micro-swimmers actuated by responsive gel. *Soft Matt.* **8**, 8944–8951.

MO, G. B. & SANGANI, A. S. 1994 A method for computing Stokes flow interactions among spherical objects and its application to suspensions of drops and porous particles. *Phys. Fluids* **6**, 1637–1652.

NGUYEN, H., KARP-BOSS, L., JUMARS, P. A. & FAUCI, L. 2011 Hydrodynamic effects of spines: A different spin. *Limnol. Oceanogr.-Fluids Environ.* **1**, 110–119.

OLLILA, S. T. T., ALA-NISSILA, T. & DENNISTON, C. 2012 Hydrodynamic forces on steady and oscillating porous particles. *J. Fluid Mech.* **709**, 123–148.

POZRIKIDIS, C. 1992 *Boundary Integral and Singularity Methods for Linearized Viscous Flow*. Cambridge University Press.

REGNIER, F. E. 1991 Perfusion chromatography. *Nature* **350**, 634–635.

REULAND, P., FELDERHOF, B. U. & JONES, R. B. 1978 Hydrodynamic interaction of two spherically symmetric polymers. *Physica* A **93**, 465–475.

RICHARDSON, J. & POWER, H. 1996 A boundary element analysis of creeping flow past two porous bodies of arbitrary shape. *Engng Anal. Bound. Elem.* **17**, 193–204.

SONNTAG, R. C. & RUSSEL, W. B. 1987 Structure and breakup of flocs subjected to fluid stresses. II. Theory. *J. Colloid Interface Sci.* **115**, 378–389.

STUART, M. A. C., HUCK, W. T. S., GENZER, J., MULLER, M., OBER, C., STAMM, M., SUKHORUKOV, G. B., SZLEIFER, I., TSUKRUK, V. V., URBAN, M., WINNIK, F., ZAUSCHER, S., LUZINOV, I. & MINKO, S. 2010 Emerging applications of stimuli-responsive polymer materials. *Nat. Mater.* **9**, 101–113.

VAINSHTEIN, P. & SHAPIRO, M. 2006 Porous agglomerates in the general linear flow field. *J. Colloid Interface Sci.* **298**, 183–191.

VAINSHTEIN, P., SHAPIRO, M. & GUTFINGER, C. 2004 Mobility of permeable aggregates: effects of shape and porosity. *J. Aerosol Sci.* **35**, 383–404.

VANNI, M. & GASTALDI, A. 2011 Hydrodynamic forces and critical stresses in low-density aggregates under shear flow. *Langmuir* **27**, 12822–12833.

YANG, S. M. & HONG, W. H. 1988 Motions of a porous particle in Stokes flow. Part 1. Unbounded single-fluid domain problem. *Korean J. Chem. Engng* **5**, 23–34.

YANO, H., KIEDA, A. & MIZUNO, I. 1991 The fundamental solution of Brinkman equation in 2 dimensions. *Fluid Dyn. Res.* **7**, 109–118.

ZLATANOVSKI, T. 1999 Axisymmetric creeping flow past a porous prolate spheroidal particle using the Brinkman model. *Q. J. Mech. Appl. Maths* **52**, 111–126.